JPE 12-3-5

http://dx.doi.org/10.6113/JPE.2012.12.3.418

Improving the Overall Efficiency for DC/DC Converter with LoV-HiC System

Dong-Hwa Han*, Young-Jin Lee*, Wan-Sung Kwon*, Mohammed A. Bou-Rabee**, and Gyu-Ha Choe†*

†*Dept. of Electrical Eng., Konkuk University, Seoul, Korea
**PAAET Dept. of Electrical Eng., College of Technological Studies, Kuwait

Abstract

It is very important to improve the overall efficiency of systems with a source of power that has low-voltage high-current terminal characteristics such as fuel cells. A resonant converter is required for high efficiency systems. However, the peak value of the switches current is large in a resonant converter. This peak current requires a large number of switches and results in system failures. In this paper, an analysis and experiments of a resonant isolation push-pull converter are performed. A switching loss analysis is performed in order to compare losses between a resonant push pull converter and a hard switching push-pull converter. Specially, the conduction loss is studied based on the ratio between the resonant frequency and the switching frequency. In addition, a method for improving the efficiency is implemented with conventional HF insolation converters.

Key words: Full-Bridge, Hard switching, LoV-HiC system, Push-Pull, Resonant Converter, Soft switching

I. INTRODUCTION

Nowadays, the interest in clean energy has been focused all over the world because of environmental pollution caused by the fossil fuels. Solar, wind, fuel and biomass are promising sources of clean energy. Moreover, the Korean government has declared a policy of 'Lower carbon and Green growth' for the national development of renewable energy. The usable output of wind and solar energies is dependent of environmental conditions such as the weather, the wind speed and the insolation level. However, regardless of these external conditions, the output energy can be maintained at an acceptable level with fuel cell systems. At the moment, renewable energy sources such as FC (Fuel Cell) energy with hydrogen fuel can be regarded as the most promising for use in the near future. However, a fuel cell stack has a relatively low voltage and a high current, plus the characteristic of a large voltage drop when increasing the current.[1]-[5] A FC stack can be regarded as a low-voltage high-current (LoV-HiC) system. Recently, a lot of development has been done on inverters. As a result inverters with an efficiency of 95% are available on the global market. However, most of converters have an efficiency that is lower than 90%, which means that they need to be developed to achieve a higher efficiency.[6] In a LoV-HiC PCS (Power Conditioning System), the DC/DC converters are classified into four typical types: non-isolated boost converters, isolated converters, two-stage converters and PISO connection resonant converters. In a non-isolated boost converter, a single non-isolated boost converter results in a large input current ripple, and hence an interleaved non-isolated boost converter is used for reducing the current ripple.[7~9] Also in an isolated converter a line frequency transformer should be used for the galvanic isolation between the input and the output, which could cause disadvantages such as a high cost and a large volume. HF (high-frequency) isolated converters of the FB (Full-Bridge) and PP (Push-Pull) types can be used to overcome these disadvantages. Since these converters are hard-switching, their efficiency is relatively low.[10]-[14] For higher efficiency resonant type converters are needed. However, it is not easy to apply a resonant converter to LoV-HiC systems such as fuel cells because a resonant converter with a fixed duty cannot control the output voltage. Therefore there are two choices for controlling the output voltage: the two-stage converter and the PISO (Parallel-Input Series-Output) converter structures. In the two-stage converter the output can be controlled by hard switching the boost converter, but the efficiency becomes lower because of hard-switching [15]. The PISO structure is

Manuscript received Apr. 21, 2011; revised Mar. 29, 2012
Recommended for publication by Associate Editor Woo-Jin Choi.
†Corresponding Author ghchoe@konkuk.ac.kr
Tel: +82-2-450-3486, Fax: +82-2-447-9186, Konkuk University
*Dept. of Electrical Eng., Konkuk University, Seoul, Korea

composed of several fixed-duty resonant converters, which maintain the DC link voltage level to within an acceptable range by changing the connection of the converters according to the different input voltages [16].

Since the PISO structure has the same circuit as the dc resonant topology, a single DC/DC resonant converter is designed and analyzed in this paper. A 1 kW resonant push-pull (PP) converter is theoretically investigated and then experimentally implemented. In addition, a loss analysis is studied and compared to the resonant push-pull converter and hard-switching converters in various schemes for improving the overall efficiency. Also a factor K is suggested to investigate the relationship between the switching frequency and the resonant frequency for the conduction loss of switches. Finally, the overall efficiency of the resonant converter is found and then compared with the those of different hard-switching converters. In the resonant PP converter, the characteristic of high efficiency can be shown and proven theoretically and experimentally.

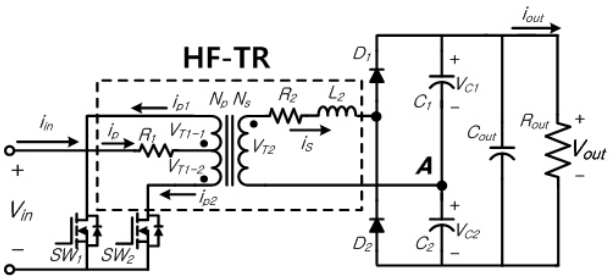

Fig. 1. Power circuit of resonant push-pull converter.

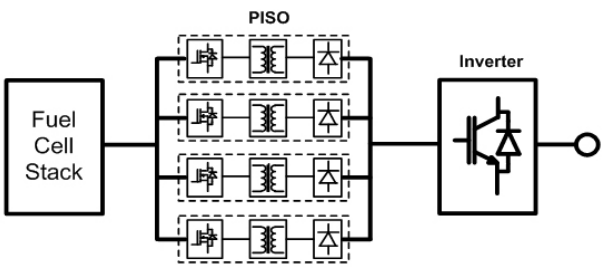

Fig. 2. The PISO system with fuel cell of LoV-HiC.

II. RESONANT PUSH-PULL CONVERTER

A. Basic Structure

Fig. 1 shows the power circuit of the resonant push-pull converter topology studied in this paper. It consists of a resonant push-pull converter and a voltage doubling circuit. The former is composed of two MOSFET switches, which enable the magnitude of the output voltage, V_{out}. The latter is composed of two diodes and two capacitors rather than four diodes. The voltage doubling circuit makes the output voltage, V_{out} becomes doubled by two series-connected capacitors. In addition, the HF transformer has a center tap at the primary winding of push-pull type. The circuit topology for this resonant push-pull converter is quite similar to that of a switching-type PP converters. For making resonance, the internal leakage reactance of the HF transformer is used instead of an external inductor. The high-frequency capacitors C_1 and C_2 have two functions; voltage-doubling and circuit-oscillating. [17]-[19]

The resonant frequency becomes $f_r = \frac{1}{2\pi\sqrt{L_2 C_r}}$ and the switching frequency of the resonant push-pull converter is defined as f_{sw}. The switching frequency should be chosen as $f_{sw} \le f_r$ to ensure the resonant operation. It is important to determine the leakage inductance of the HF transformer, which can be regarded as a physical structure such as the core, winding, gap size, and thickness of the isolation between the conductors.

B. Proposed PISO Structure

To operate an inverter stably its DC link voltage should be maintained within an acceptable range. However, because a resonant converter cannot control its output voltage or the DC link voltage of the inverter, a special structure such as a PISO connection can be considered as in Fig. 2. Its structure can be determined according to several factors such as variations of the input voltage, the loading conditions, the number of resonant converters, the transformer ratio and the allocated power capacity. The connection of four resonant converters should be made considering these factors. For example, four outputs of 180[V], 90[V], 60[V], 30[V] can be set to get a DC voltage of 360[V]. In addition, it is possible to do this with three outputs of 240[V], 80[V], 40[V] with a different input voltage.

III. CIRCUIT ANALYSIS

Each converter of the PISO connection in Fig. 2 has the same circuit topology as the resonant push-pull type. As a result, the analysis for a resonant push-pull converter can be made in this paper. Suppose that the energy is charged completely at the output capacitor C_{out} of Fig. 1 and that the output voltage, V_{out} becomes almost constant by a large capacitance. The output voltage can then be expressed as (1).

$$v_{c1}(t) + v_{c2}(t) = V_{out} \tag{1}$$

When the switch SW_1 is turned on at t = 0, the waveform of Fig. 3(b), $v_{T1-1}(t)$ appears at the primary side of the HF step-up transformer. Therefore, the secondary voltage $v_{T2}(t)$ becomes a square wave, as in Fig. 3(c), which is applied to a loop composed of the secondary winding resistance R_2, the leakage inductance L_2, diode D_1 and capacitor C_1.

The following expression of $v_{T2}(t)$ is obtained since V_{D1} is negligible: ($V_{D1} = 0.7[V]$)

$$v_{T2}(t) = R_2 i_s(t) + L_2 \frac{di_s(t)}{dt} + v_{c1}(t) \quad (2)$$

A. Secondary and Primary Transformer Currents

To find the secondary current $i_s(t)$, it is necessary to get the relationship between the capacitor voltage and the secondary current $i_s(t)$. If the Kirchhoff current law is applied to node A together with (1), then the relationship between $i_s(t)$ and $v_{c1}(t)$ is obtained as:

$$i_s(t) = C_1 \frac{dv_{c1}(t)}{dt} - C_2 \frac{dv_{c2}(t)}{dt} = (C_1 + C_2)\frac{dv_{c2}(t)}{dt}. \quad (3)$$

Therefore equation (2) can be expressed by using (3) as:

$$v_{T2}(t) = L_2 \frac{di_s(t)}{dt} + R_2 i_s(t) + V_{c1}(0) + \frac{1}{C_r}\int i_s(t)dt \quad (4)$$

where $C_r = C_1 + C_2$.

By differentiating (4) and then rearranging, the following equation can be obtained as:

$$\frac{d^2 i_s(t)}{dt^2} + 2\alpha \frac{di_s(t)}{dt} + \omega_r^2 i_s(t) = 0 \quad (5)$$

where $\alpha = \frac{R_2}{2L_2}$, $\omega_r = \frac{1}{\sqrt{L_2 C_r}}$.

Equation (5) should be satisfied with the condition of $\alpha^2 \ll \omega_r$, or $R_2^2 \ll \frac{4L_2}{C_1 + C_2}$ in order to make a resonance within the loop of $R_2 - L_2 - D_1 - C_1 - v_{T2}$. Hence the secondary current $i_s(t)$ can be obtained from (5) as:

$$i_s(t) = I_{mp} e^{-\alpha t} \sin(\omega_d t - \phi). \quad (6)$$

where ϕ is the phase angle, which becomes zero from the initial condition of $i_s(0) = 0$. Therefore the secondary current becomes a slightly distorted sinusoidal wave as:

$$i_s(t) = I_{mp} e^{-\alpha t} \sin \omega_d t. \quad (7)$$

In addition, the primary current $i_p(t)$ flows like the secondary current:

$$i_p(t) = \frac{N_p}{N_s} I_{mp} e^{-\alpha t} \sin \omega_d t. \quad (8)$$

Since the secondary winding resistance R_2 is actually measured as 0.1[Ω] in the experimental circuit, it can be neglected. Then both the primary and secondary currents of the HF transformer can be represented ideally as:

$$i_p(t) = \frac{N_p}{N_s} I_m \sin \omega_r t. \quad (9)$$

$$i_s(t) = I_m \sin \omega_r t. \quad (10)$$

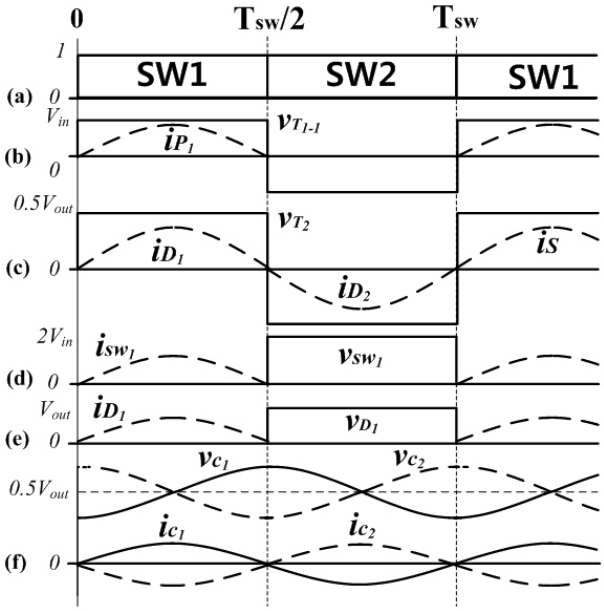

(a) The gate signal of SW_1 and SW_2.
(b) The primary voltage and current of HF transformer.
(c) The secondary voltage and current of HF transformer.
(d) The voltage and current of switch SW_1.
(e) The voltage and current of diode D_1.
(f) The voltage and current of capacitor C_1 and C_2.

Fig. 3. Voltage and current waveforms of resonant push-pull converter.

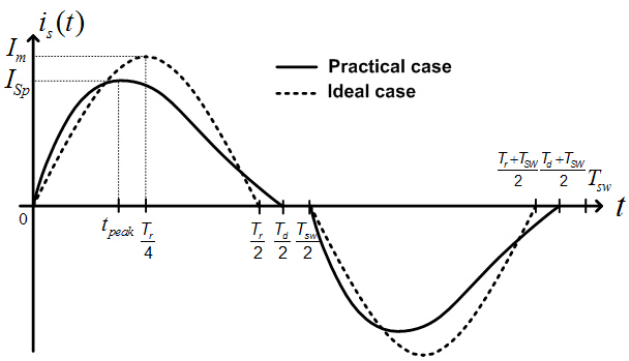

Fig. 4. A complete period of both practical and ideal secondary current.

Fig. 4 shows the waveforms of (7) and (10) during a complete switching period T_{sw}. For a given switching half period, a half period of the practical current is $T_d/2$ and a half period of the

ideal current is $T_r/2$. In order that the practical current becomes zero between $[T_d/2,\ T_{sw}/2]$, the switching period should be set and hence the relationship of $T_{sw} > T_d > T_r$ is required for the soft switching of the resonant PP converter.

Actually both currents become closely sinusoidal as shown in Fig. 4, and hence the soft switching can be achieved. As soon as the switch SW_1 is turned on at the time instant t=0, the secondary current $i_s(t)$ becomes sinusoidal, and then it stops flows at t = $T_d/2$. For the rest of the half-cycle, if the switch SW_2 is turned on at the time instant t = $T_{sw}/2$, then the current $i_s(t)$ becomes negative and then reaches zero at t = $(T_d + T_{sw})/2$. This resonant process is repeated for every cycle. Assuming the constant average I_{out} in the doubling circuit, the coefficients of secondary current $i_s(t)$ can be obtained as:

$$\text{i)}\quad \text{ideal case}: \quad I_m = \frac{\omega_r \pi}{\omega_{sw}} I_{out} \tag{11a}$$

$$\text{ii) practical case}: \quad I_{mp} = \frac{2\pi(\alpha^2 + \omega_d^2)}{\omega_{sw}\omega_d\left(1 + e^{-\frac{\alpha T_d}{2}}\right)} I_{out} \tag{11b}$$

where $T_d = \dfrac{2\pi}{\omega_d}$.

The relationship between I_{mp} and I_m is obtained as:

$$I_{mp} = \frac{T_d \omega_r}{\pi\left(1 + e^{-\frac{\alpha T_d}{2}}\right)} \cdot I_m \tag{12}$$

The peak time instant of $i_s(t)$ is obtained as:

$$t_{peak} = \frac{\tan^{-1}\left(\frac{\omega_r}{\alpha}\right)}{\omega_d}. \tag{13}$$

Therefore, the peak value I_{sp} of $i_s(t)$ can be expressed as:

$$I_{sp} = \frac{2T_d I_m e^{-\alpha\left(\frac{\tan^{-1}\left(\frac{\omega_d}{\alpha}\right)}{\omega_d}\right)}}{T_r\left(1 + e^{-\frac{\alpha T_d}{2}}\right)} \left(\sin\left(\tan^{-1}\frac{\omega_d}{\alpha}\right)\right). \tag{14}$$

B. Capacitor Voltage and Output Voltage

To find the capacitor voltage, it is necessary to know the leakage inductance of the HF transformer and also to set the switching frequency f_{sw}.

As shown in Fig. 4, the switching frequency should be set lower than the resonant frequency $f_r = \dfrac{1}{2\pi\sqrt{L_2 C_r}}$. Therefore a capacitor should be chosen that satisfies the relationship of:

$$C_r \le \frac{1}{L_2 \omega_{sw}}. \tag{15}$$

Because the secondary current $i_s(t)$ has already been found as in (7) or (10), the capacitor voltage $v_{c1}(t)$ can be obtained easily from (3).

i) ideal case : $i_s(t) = I_m \sin\omega_r t$

$$v_{c1}(t) = \frac{-I_m}{C_r \omega_r}\cos\omega_r t + V_{c1}(0) \tag{16}$$

where $V_{c1}(0) = \dfrac{1}{2}V_{out} - \dfrac{I_m}{C_r\omega_r}$

ii) practical case : $i_s(t) = I_{mp} e^{-\alpha t}\sin\omega_d t$

$$v_{c1}(t) = \frac{-I_m}{C_r \omega_r} e^{-\alpha t} sin(\omega_d t + \delta) + V_{c1}(0) \tag{17}$$

where $\delta = tan^{-1}\dfrac{\omega_d}{\alpha}$

$$V_{c1}(0) = \frac{1}{2}V_{out} - \frac{\omega_d}{C_r\omega_r}\cdot I_m \sin(\delta)$$

In addition, by differentiating (16) or (17), the capacitor current $i_{c1}(t)$ is given easily as:

$$\text{i)}\quad \text{ideal case}: \quad i_{c1}(t) = \frac{I_m}{2}\cdot\sin\omega_r t \tag{18}$$

$$\text{ii)}\quad \text{practical case}: \quad i_{c1}(t) = \frac{I_{mp}}{2} e^{-\alpha t}\sin\omega_d t \tag{19}$$

Through the above procedure, the operation of the proposed resonant PP converter is analyzed theoretically, and hence Fig. 3 describes its overall operation and several important waveforms.

Practically every capacitor voltage has an average of 178[V] with a ripple of 10[V], which means a ripple factor of 5.6%. However, the output voltage is almost constant at V_{out} (356[V]), and its ripple factor is lower than 0.015%. Because of the opposite polarity between $v_{c1}(t)$ and $v_{c2}(t)$, the ripple voltages of the output cancel each other out, which can be called self-ripple cancellation. As a result the resultant ripple becomes almost zero, and hence a minimally sized output capacitor can be used in the proposed circuit.

IV. POWER LOSS AND EFFICIENCY

A. Power Loss in a Resonant Push-Pull Converter

A resonant push-pull converter consists of four major components which consist of power switches, an HF transformer, diodes and capacitors. Table I shows the specifications of the used devices in a resonant Push-Pull converter. Loss of the four major components can be found as follows:

TABLE I

DEVICE SPECIFICATIONS OF RESONANT PUSH-PULL CONVERTER

Device	Part Number (Company)	Features
Switch	IRFP 4668(IR)	- low on resistance - high speed switching
Transformer Core	EE 7066 (ISU)	-high permeability -low loss
Diode	HFA135NH(Vishay)	-ultrafast soft recovery -Low loss
Capacitor	B32592(Epcos)	-high frequency -high pulse strength

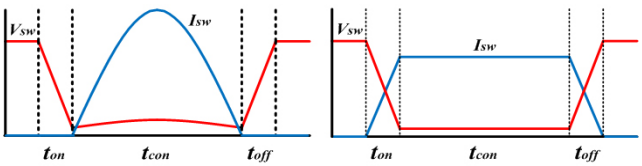

(a) resonant switching scheme (b) hard switching scheme

Fig. 5. Waveforms of switch voltage and current in the resonant and hard switching schemes.

1) Switch Loss

In Fig. 5, the losses of the hard switching scheme are defined as the sum of the on-transient, off-transient and conduction losses. So the switch loss of the hard switching scheme can be expressed as:

$$P_{SW}{}^{H} = P_{on} + P_{conH} + P_{off} \tag{20}$$

where:

$$\text{on-transient loss} \quad P_{on} = \frac{1}{2} \cdot V_{sw} \cdot I_{sw} \cdot f_{sw} \cdot t_{on}$$

$$\text{conduction loss} \quad P_{conH} = I_{sw}{}^{2} \cdot R_{ds} \cdot f_{sw} \cdot t_{con}$$

$$\text{off-transient loss} \quad P_{off} = \frac{1}{2} \cdot V_{sw} \cdot I_{sw} \cdot f_{sw} \cdot t_{off} \quad . \tag{21}$$

and t_{on} = turn-on transient time,

t_{con} = conduction time,

t_{off} = turn-off transient time.

However, the switch current flows in a sinusoidal form, as shown in Fig. 3(d). The on/off transient losses are ignored because they are very small. Since the switch current $i_{sw1}(t)$ is equal to the primary current $i_{p1}(t)$, the power loss of SW_1 is $I_{sw1}^2 \cdot R_{ds}$ (Here, R_{ds} is the MOSFET on-resistance). In addition, for the negative cycle, the switch SW_2 is turned on to generate the power loss of SW_2 and hence the switch loss P_{sw} for one complete period is expressed as:

$$P_{sw} = P_{sw1} + P_{sw2} \, . \tag{22}$$

Here (IRFP 4668, IR) Power MOSFETs are chosen due to their high speed power switching and low on-resistance.

2) Diode Loss

The general loss equation in a diode can be expressed as:

$$P_D = (V_D \times I_D + I_D{}^2 \cdot R_d) \cdot f_{sw} \cdot t_{con} \, . \tag{23}$$

Here R_{ds} is the Diode on-resistance, by which the loss can be ignored. The diode current $i_{D1}(t)$ becomes the positive half-cycle of the secondary current of the HF transformer, as shown in Fig. 3(c). Therefore, the sum of the two diode currents is equal to the secondary current. In addition, the diode voltage drop V_D becomes roughly 0.7[V]. Since the loss of the diode D_1 is $(0.7) \cdot I_{D1}$, the diode losses are given as:

$$P_D = 2 \cdot V_D \cdot I_{D1} = 1.4 I_{D1} \, . \tag{24}$$

The diodes used are the ultrafast soft recovery type (HFA135NH, Vishay), which have a very low Q_{rr} (Reverse recovery charge) and T_{rr} (Reverse recovery time). The characteristics are very good for reducing losses and EMI/RFI in high frequency SMPS [20].

3) HF Transformer Loss

The HF transformer losses P_{TR} are divided into copper loss P_C and iron loss P_{h+e}. These relationships are summarized as:

$$P_{TR} = P_C + P_{h+e} \tag{25}$$

Where $P_{h+e} = K \cdot f^{m} \cdot B^{n}$

$$P_C = R_1 \cdot I_p{}^2 + R_2 \cdot I_s{}^2 \, .$$

An EE type transformer core (EE7066, ISU) is selected due to its high permeability and low loss characteristics. In addition, it has a primary winding of 5 turns, and a secondary winding of 18.5 turns. Hence the turn ratio is set to 0.27. Also litz wire is used to reduce the copper loss.

4) Capacitor Loss

The two capacitor currents have the same waveform but opposite polarities, as can be seen in Fig. 3(f). Let the equivalent series resistance (ESR) be equal to R_{c1} and R_{c2} respectively. Then the capacitor losses can be represented as:

$$P_C = I_{c1}^2 \cdot R_{c1} + I_{c2}^2 \cdot R_{c2} \, . \tag{26}$$

Here metalized polyester film (B32592) type capacitors are chosen for high-frequency use. Therefore, the total losses can be expressed as:

$$P_{loss} = P_{SW} + P_D + P_{TR} + P_C \, . \tag{27}$$

Therefore the efficiency η of the resonant PP converter can be found as:

$$\eta = \frac{P_{in} - P_{loss}}{P_{in}} \cdot 100[\%] \quad (28)$$

where $P_{in} = V_{in} \cdot I_{in}$.

B. Generalized Analysis of the Switch Conduction Loss in a Resonant Push-Pull Converter

The conduction loss of a resonant PP converter is larger than that of hard switching converters because of its larger current. Here, the switch current of the resonant PP converter is represented as:

i) ideal case : $i_{SW1}(t) = I_{sw} sin\omega_r t$ (29a)

ii) practical case : $i_{SW1}(t) = I_{swp} e^{-\alpha t} sin\omega_d t$ (29b)

The hard switching current in the conduction time is defined as I_H. The average value in the conduction time can be represented as (30), which is for finding the average resonant switching current in the conduction time.

$$\frac{1}{T_{sw}/2} \int_0^{T_r/2} i_{SW1}(t)dt = \frac{1}{T_{sw}/2} \int_0^{T_S/2} I_H dt \quad (30)$$

From (30), the coefficients of the switch current are represented as:

i) ideal case : $I_{sw} = \frac{\omega_r \pi}{2\omega_{sw}} I_H$ (31a)

ii) practical case : $I_{swp} = \frac{\pi(\omega_r{}^2)}{\omega_{sw} \cdot \omega_d (1 + e^{-\frac{\alpha T_d}{2}})} I_H$ (31b)

The average loss of the hard switching conduction time $[0 \sim T_{sw}/2]$ can be expressed as (32), which is for comparing the resonant to the hard switching conduction loss.

$$P_{conH} = \frac{1}{T_{sw}/2} \int_0^{T_{SW}/2} (I_H)^2 R_{ds} dt = I_H{}^2 R_{ds} \quad (32)$$

In addition, the average loss of the resonant switching conduction time $[0, T_{sw}/2]$ can be expressed as:

i) ideal case : $P_{conR} = \frac{I_{sw}{}^2 \cdot R_{ds} \cdot \omega_{sw}}{2\omega_r}$ (33a)

ii) practical case :

$$P_{conR} = \frac{I_{swp}{}^2 \cdot R_{ds} \cdot \omega_{sw} \cdot \left(1 - e^{-\alpha T d}\right)}{4\pi} \left(\frac{1}{\alpha} - \frac{\alpha}{\alpha^2 + \omega_d{}^2} \right) \quad (33b)$$

Through (31) and (33) the peak value of the resonant switching current is increased by $\frac{\omega_r \pi}{2\omega_{sw}}$ times that of the hard switching,

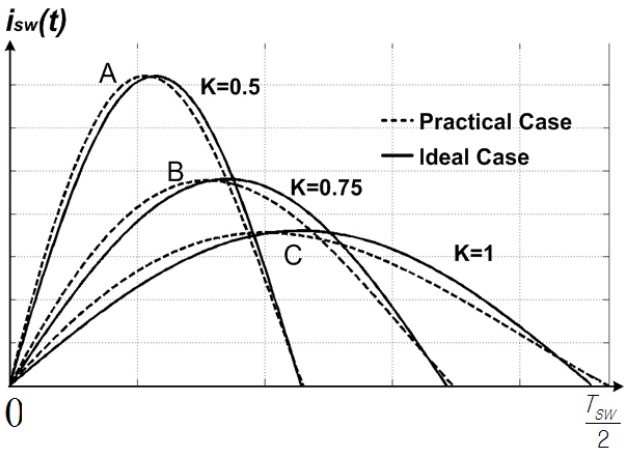

Fig. 6. Variation of switch current by K factor.

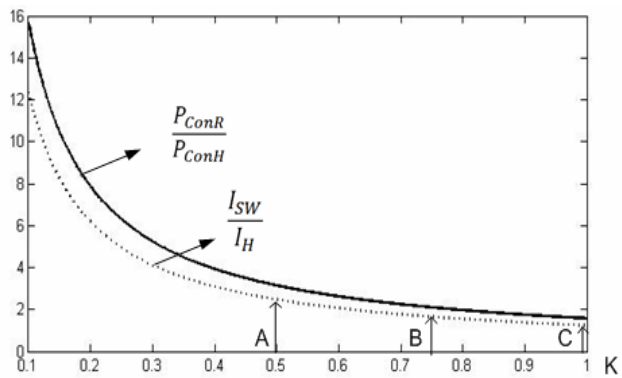

Fig. 7. Conduction loss and peak current value of the switches by K factor.

while the conduction loss of resonant switching current is increased by $\frac{\pi^2 \omega_r}{8\omega_{sw}}$ times.

1) Conduction Loss by the K factor: For finding the conduction loss of the resonant switching by variation of the switching frequency, the ratio of the switching frequency and the resonant frequency is defined as *K*, which can be expressed as:

i) ideal case : $K = \frac{\omega_{sw}}{\omega_r}$ (34a)

ii) practical case : $K = \frac{\omega_{sw}}{\omega_d}$ (34b)

The switch current shown in Fig. 6 is expressed by I_H as:

i) ideal case : $I_{sw} = \frac{\pi}{2K} I_H$ (35a)

ii) practical case : $I_{swp} = \frac{\pi \cdot (\omega_r{}^2)}{K \cdot \omega_d{}^2 \cdot (e^{-\frac{\alpha T_d}{2}} + 1)} I_H$ (35b)

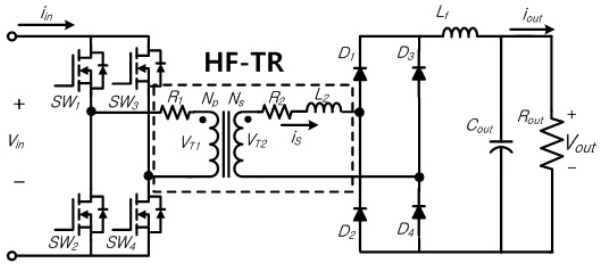

(a) Full-Bridge Converter.

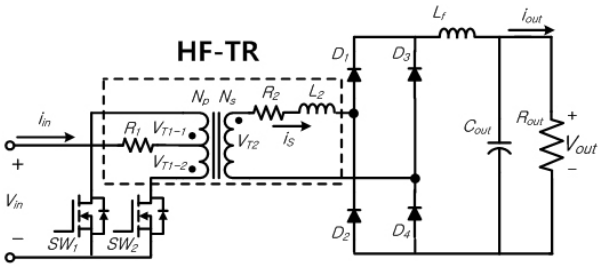

(b) Push-Pull Converter.

Fig. 8. Hard switching type converters.

Here, the conduction loss by K can be expressed as:

$$\text{i)} \quad \text{ideal case}: \quad P_{conR} = \frac{K}{2} I_{sw}^2 R_{ds} \tag{36a}$$

ii) practical case :

$$P_{conR} = \frac{K \cdot {I_{swp}}^2 \cdot R_{ds} \cdot \omega_d \cdot \left(1 - e^{-\alpha T d}\right)}{4\pi} \left(\frac{1}{\alpha} - \frac{\alpha}{\alpha^2 + {\omega_d}^2} \right) \tag{36b}$$

2) Considerations on the Switching Frequency: The switching frequency is an important factor for the stable and efficient operation of a system. This is because the switching frequency is changed with the peak value of the switch current. The timing waveform of the switch current is changed by *K* as in Fig. 6, but the average values are unchanged. The solid line means the ratio of $\frac{P_{conR}}{P_{conH}}$, which represents *K* and should as low as possible to reduce the power loss of the resonant current. The conduction loss is inversely proportional to *K*. The dotted line of Fig. 7 represents the peak value of the transformer primary current as a factor of *K*. The switch current becomes reduced to 3.14, 2, and 1.57 for each *K* of 0.5, 0.75 and 1.0. The larger current can damage the switches and result in transformer saturation. For a stable and high efficiency DC/DC converter, the switching frequency should be set near the resonant frequency. In addition, the practical resonant frequency is a little lower than ideal case. Therefore, the switching frequency should be set through repeated experimentation.

C. Loss Comparison of Different Converters

FB and PP converters of the hard switching type are studied and then compared with a PP converter of the soft switching type.

TABLE II

SIMULATION PARAMETERS OF RESONANT PP CONVERTER

Vin	50[V]
Output Power	1000[W]
Equivalent resistance	144.4[Ω]
Switching frequency	21.5[kHz]
Resonant frequency	22[kHz]

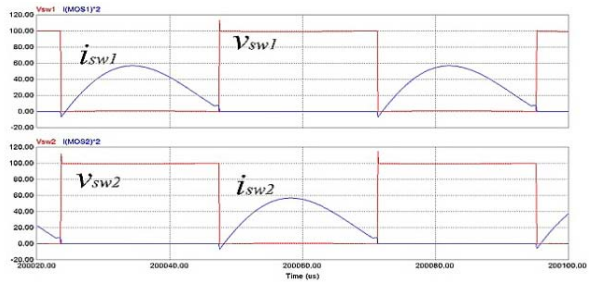

(a) waveforms of switches.

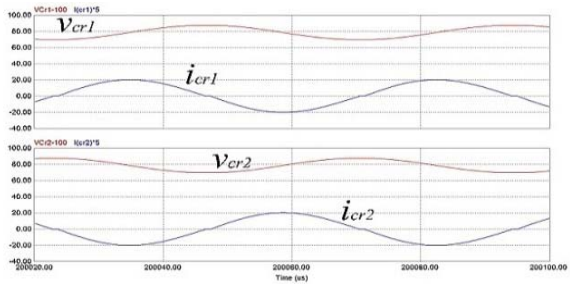

(b) waveforms of capacitors.

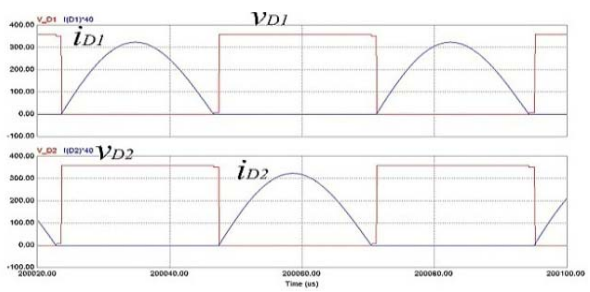

(c) waveforms of diodes.

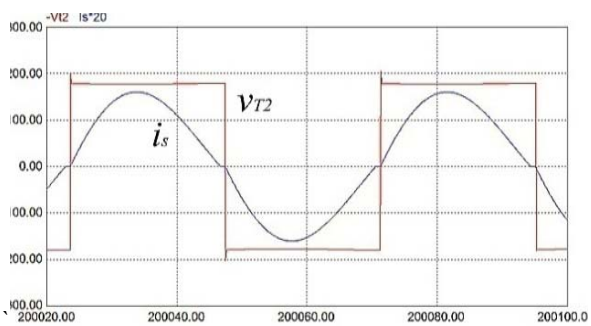

(d) waveforms of transformer.

Fig. 9. Waveforms of resonant push-pull converter.

TABLE III

DEVICE SPECIFICATIONS OF RESONANT PUSH-PULL CONVERTER

Converter Loss	Resonant Push-Pull converter
P_{sw}	0.195
P_{Tr}	0.65
P_D	0.14
P_C	0.03
P_{total}	1

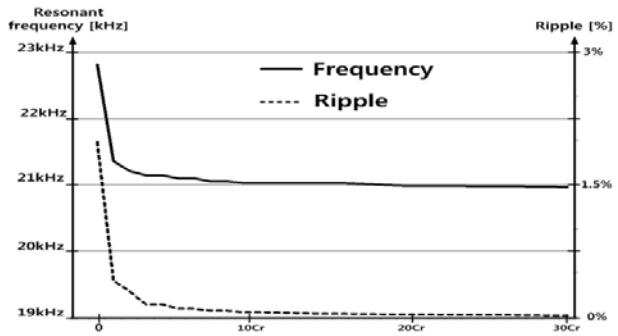

Fig. 10. The relationship of resonant frequency and ripple by the variation of output capacitor.

The circuit parameters are listed as follows:

- rated input voltage V_{in} =50[V]
- rated input current I_{in} =20[A]
- switching frequency f_{sw} =20[kHz]
- MOSFET (IRFP 4668) R_{ds} =8.0[mΩ]

V. SIMULATION AND EXPERIMENT

A. Simulation of a Resonant Push-Pull converter

All of the systems studied here are simulated by the PSIM (Simulation tool - PowerSim, Ver 6.0), and the parameters of the simulation are shown in the Table II.

Through the simulation, the current waveforms of the HF transformer secondary, diode and switches are obtained, as can be seen in Fig. 9. Therefore, the voltage and current do not overlap at the turn-on and turn-off points. To avoid an infinite input current, the dead time Δ is set to 2% of one period (actually 0.93[μsec]). If both of the switches are under the turn-on state, the magnetic fields of the HF transformer cancelled each other out. Hence the input current flows only at the MOSFET's low on-resistance. The relationship between C_{out} and the resonance frequency is simulated, as can be seen in Fig. 10. When increasing the output capacitor, the frequency of the transformer secondary current f_d is decreased. If the output capacitor is set to a value larger than $6C_r$, the frequency is kept at an almost constant frequency of 21kHz. In addition, the ripple of the output voltage is simulated by the variation of the output capacitor C_{out} as in Fig. 10.

The ripple is kept lower than 1[%] when the output capacitor is more than $5C_r$. Therefore, output capacitor can be designed to have a small value while keeping a low ripple. The normalized loss in the resonant PP converter is shown in Table III. In the resonant PP converter, the largest loss is dissipated at the transformer and the secondary largest loss is at the switches.

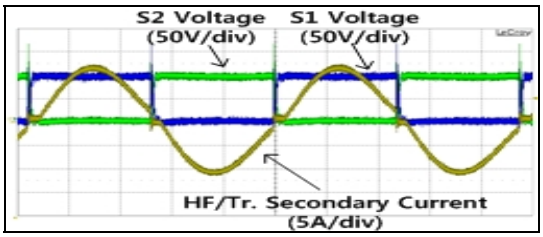

(a) Switch voltage and transformer secondary current

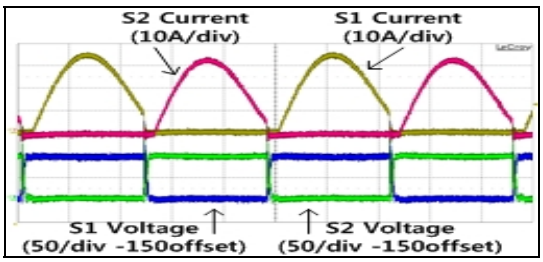

(b) Voltage and current of the switches

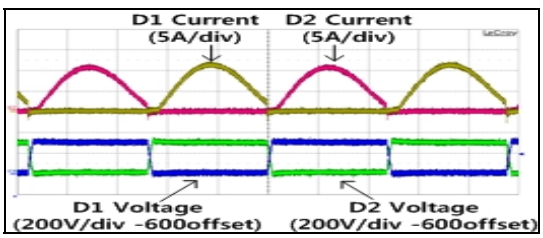

(c) Voltage and current of the diode

Fig. 11. Waveforms of Resonant Push-Pull Converter.

B. Experiment on a Resonant Push-Pull converter

The efficiency and resonant characteristics are evaluated at the rated input voltage (Vin =50[V]) according to variations of the load. The efficiency is measured by a PM3000A (Voltech–power analyzer). And the waveform is captured by a Waverunner (Recroy-scope). The voltage and current waveforms of the resonant push-pull converter are shown in Fig. 11. It can be seen that the currents of the switches, transformer and diodes become almost sinusoidal. As with the previous simulation result, an overlap (between the voltage and the current) does not occur. In Fig. 11, the current waveforms of the switches are different from each other. This is caused by the leakage inductance of the primary winding, since the two windings of the primary side are not exactly equal to each other. This is not an important defect of the system operation.

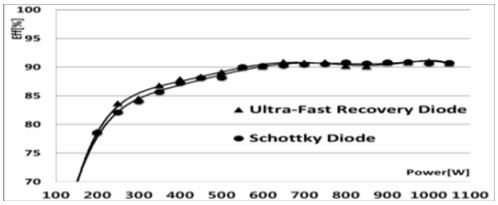

(a) Different diodes.

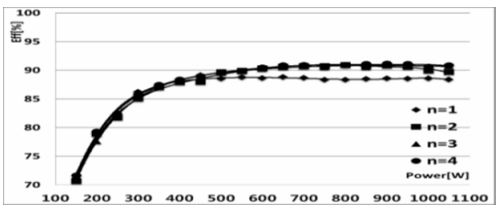

(b) Number of parallel switches.

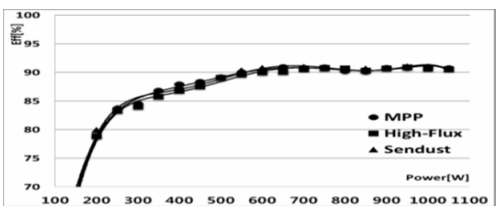

(c) Different cores.

Fig. 12. Variation of efficiency to different diodes, cores, number of parallel switches at Push-Pull Converter.

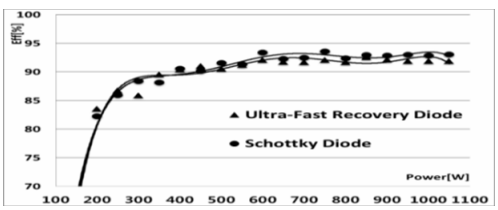

(a) Different diodes.

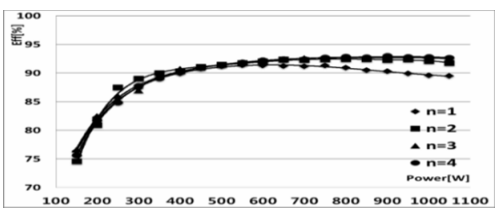

(b) Number of parallel switches.

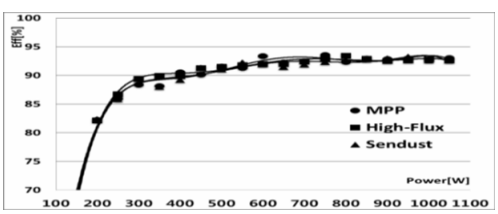

(c) Different cores.

Fig. 13. Variation of efficiency to different diodes, cores, number of parallel switches at Full-Bridge Converter.

TABLE IV

COMPARISON OF SWITCHING LOSSES AT DIFFERENT CONVERTERS

Converter / Loss	Hard switching		Soft switching
	FB Type	PP Type	Resonant PP Type
On-transient Loss P_{on}	0.14	0.18(0.1)	-
Off-transient Loss P_{off}	0.18	0.21(0.12)	-
Conduction Loss P_{con}	0.68	0.61(0.35)	1(0.44)
P_{sw}	1	1(0.57)	1(0.44)

*( ) = Normalized by P_{sw} of Full-bridge converter

TABLE V

COMPARISON OF TOTAL LOSSES AT DIFFERENT CONVERTERS

Converter / Loss	Hard switching		Soft switching
	FB Type	PP Type	Resonant PP Type
P_{sw}	0.17	0.12(0.106)	0.195(0.086)
P_{Tr}	0.54	0.56(0.497)	0.65(0.288)
P_D	0.09	0.1(0.088)	0.14(0.062)
P_C	0.02	0.03(0.026)	0.03(0.0133)
P_L	0.18	0.19(0.168)	-
P_{total}	1	1(0.888)	1(0.445)

*( ) = Normalized by P_{total} of Full-bridge converter

C. Improving efficiency in Hard switching Type Converters

The main components of the losses in the hard switching converter of a PP converter and a FB converter can be classified as follows: the diode, the switch (MOSFET) and the core. To improve the efficiency, the ultra-soft diode is replaced by a Schottky diode in the rectifier circuit. In addition, the MOSFET's are connected in parallel, and the inductor core of the filter is changed. As can be seen in Fig. 12(a) and Fig. 13(a), as a result of the changed Schottky diode, the efficiency is improved by approximately 3% in the full-bridge converter, which is caused by the zero reverse recovery time in the Schotty diode. By paralleling the MOSFET's, as in Fig. 12(b) and Fig. 13(b), the efficiency is improved by roughly 1~1.5% in the FB and PP converters. However, there is no big difference when comparing the paralleling of two and four MOSFETs. Therefore, the paralleling of two MOSFET's is suitable and recommended in terms of size, volume and price. When changing the inductor cores (MPP, Sendust, High-flux), as in Fig. 12(c) and Fig. 13(c), the efficiency improvement is not large. In the experiment result, the FB converter is shown to have a 93% (approximately 3% increase) converter efficiency. However, that requires to many improvements when considering the efficiency of the whole system.

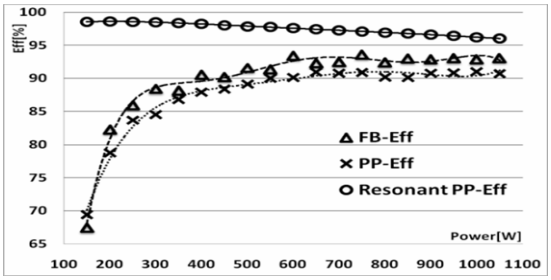

Fig. 14. Efficiency Comparison of Converters.

Table IV shows a comparison of the switch loss. The switch loss in the PP converter is small because it has fewer switches than the FB converter. In addition, the switch loss of the resonant converter is 44% of the FB converter loss. Table V expresses the total loss of the converters. In the hard switching converter type, the efficiencies of the FB converter and the PP converter are measured at 90.06%, 91.12% respectively.

In the comparison of the hard switching converters and the resonant PP converter, the resonant PP converter has a higher efficiency characteristics under the light load condition. It appears to be higher than 96% efficiency under any loading conditions, as can be seen in Fig. 14.

VI. CONCLUSIONS

In this paper, operation and loss analysis are carried out on a resonant isolation push-pull converter. The switching loss analysis is performed in order to compare the losses between the resonant push pull converter and a hard switching push-pull converter. In particular, the ratio of the switching frequency and the resonant frequency *K* is suggested for the analysis of the conduction loss and the peak current value in the resonant PP converter. In addition, the conduction loss of the switch and the peak value of the current are obtained by the *K* factor. This can be utilized to design the relationship between the switching frequency and the resonant frequency in the resonant converter. Through experiments on a resonant PP converter, the efficiency is kept above 96[%] under all load conditions. The superiority of the resonant PP converter over the conventional HF isolation converter is proven through circuit analysis, simulations and experiments for LoV-HiC systems such as fuel cells.

ACKNOWLEDGMENT

This paper was supported by Konkuk University in 2009. The authors would like to thank Konkuk University for supporting the research fund and the help related to this research.

REFERENCES

[1] J. Rifkin, *The hydrogen Economy*, Tarcher Putnam, 2002.

[2] R. O'Hayre, *Fuel cell Fundamental*, 1st edition Wiley & Sons, 2006.

[3] G. Hooger, *FUEL CELL Technology Handbook*, CRC Press, 2003.

[4] S. Obara , *Fuel cell Micro-grids*, 1st edition, Springer, 2009.

[5] A. Emadi and S. S. Williamson "Status review of power electronic converters for fuel cell applications," *Journal of Power Electronics*, Vol. 1, No. 2, pp. 133-144, Oct. 2001.

[6] M. Nehrir and C. Wang, *Modeling and control of Fuel cell*, 1st Edition, John Wiley & sons, pp. 269-272, 2009.

[7] J. Lee, S. Choe, J. Ahn, and S. Baek, "Modeling and simulation of a polymer electrolyte membrane fuel cell system with a PWM DC/DC converter for stationary applications," *Power Electronics IET*, Vol. 1, pp.305-317, 2008.

[8] G. Sukumara, A. Parthasarathy, and V. Shankar, "Fuel cell based uninterrupted power sources," *Power Electronics and Drive Systems International Conf.*, Vol. 2, pp.728-733, 1997.

[9] T. Asaeda, "DC-to-AC Power Converter for Fuel Cell System," *Telecommunications Energy Conference,* pp.84-91, 1983.

[10] S. Igarashi, K. Kuroki, Y. Hatta, and H. Mogi, "Interconnection inverter consisting of large capacity DC/DC converter and HF PWM inverter fuel cell power plant," *Power Electronics and Motion Control International Conf.*, Vol. 1 , pp.196-201, 1992.

[11] M. Mohr and F. Fuchs, "Voltage fed and current fed full bridge converter for the use in three phase grid connected fuel cell systems," *Power Electronics and Motion Control Conf. IPEMC,* Vol. 1, pp. 1-7, 2006.

[12] M. Ordonez and J. Quaicoe, "Soft-switching techniques for efficiency gains in full-bridge fuel cell power conversion," *IEEE Trans. Power Electron.*, Vol. 26, No. 2, pp. 482-492, Feb. 2011.

[13] S.-K. Kwon, and K. F. A. Sayed "Boost-Half Bridge Single Power Stage PWM DC-DC Converters for PEM-Fuel Cell Stacks," *Journal of Power Electronics*, Vol. 8, No.3, pp. 239-247, Jul. 2008.

[14] L. Zhang , X. Yang, W. Chen, and X. Yao "An isolated soft-switching bidirectional buck-boost inverter for fuel cell applications," *Journal of Power Electronics*, Vol. 10, No. 3, pp.235-244, May 2010.

[15] B. Han, J. Lee, and Y. Jeong, "Power conditioning system for fuel cell with 2-stage DC-DC converter," *Applied Power Electronics Conf.,* pp. 303-308, 2010.

[16] D. Han , Y. Lee, B. Jeong, and G. Choe, "Multi-level resonant push-pull converter for fuel cell system," *Power Electronics and ECCE Asia (ICPE & ECCE), 2011 IEEE 8th International Conf.,* ,pp. 1901-1907, 2011.

[17] J. Peng, F. Anderson, J. Joseph, and A. Buffenbarger, "Low cost fuel cell converter system for residential power generation," IEEE Trans. Power Electron., Vol. 19, pp. 1315-1322, Sep. 2004.

[18] Y. Gu, L. Hang, Z. Lu, Z. Qian, and D. Xu, "Voltage Doubler Application in Isolated Resonant Converters," *Industrial Electronics Society IECONAnnual Conf.*, pp, 375-380, 2005.

[19] C. Kim, G. Moon, and S. Han "Voltage doubler rectified boost integrated half bridge (vdrbhb) converter for digital car audio amplifiers," *IEEE Trans. on Power Electron.,* Vol. 22, No. 6, pp. 2321-23301 Nov. 2007.

[20] International Rectifier Datasheet, HFA135NH40 Ultrafast soft Recovery diode, 1999

Dong-Hwa Han was born in Gokseong, Korea in 1982. He received his B.S. and M.S. in Electrical Engineering from Konkuk University, Seoul, Korea, in 2008 and 2010, respectively. He is currently pursuing his Ph.D. at Konkuk University. His current research interests include the design and analysis of resonant converters and PWM inverters, PCSs related to new and renewable energy sources such as PV, fuel cells, and BESS, as well as DSP design and control.

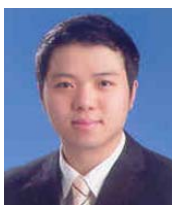

Young-Jin Lee was born in Anyang, Korea in 1982. He received his B.S. and M.S. in Electrical Engineering from Konkuk University, Seoul, Korea, in 2008 and 2010, respectively. He is currently pursuing his Ph.D. at Konkuk University. His current research interests include the design and analysis of PWM inverters, PCSs related to new and renewable energy sources, battery chargers, BESS, DC distribution, as well as DSP design and control.

Wan-Sung Kwon was born in Seoul, Korea in 1981. He received his M.S. in Electrical Engineering from Konkuk University, Seoul, Korea, in 2009. He is currently pursuing his Ph.D. at Konkuk University. His current research interests include arc fault detection algorithms, surge protection algorithms and PCSs related to new and renewable energy sources such as PV and fuel cells.

Mohammed A. Bou-Rabee was born in Kuwait in 1954. He received his B.E. in Electrical Engineering from Wichita State University, Kansas, USA, in 1984 and his M.S. in Electrical Engineering from North Carolina A&T State University, USA, in 1986. He received his Ph.D. in Electrical Engineering from The University of New South Wales, Australia, in 1992. He is currently an Assistant Professor in the Department of Electrical Engineering, PAAET College of Technological Studies, Kuwait.

Gyu-Ha Choe was born in Busan, Korea. He received his B.S., M.S., and Ph.D. in Electrical Engineering from Seoul National University, Seoul, Korea, in 1978, 1980, and 1986 respectively. Since 1980, he has been a Professor at Konkuk University, Seoul, Korea. He was a President of the Korean Institute of Power Electronics during 2007~2008. He was a Visiting Professor at Virginia Tech, USA in 1998 and at Huree University, Ulaanbatar, Mongolia. His current research interests include the application of resonant converters and PWM inverters, PCSs related to new and renewable energy sources such as PV, fuel cells, and BESS, as well as battery chargers, DC distribution, and Arc detection algorithms.